DOI: 10.19884/j.1672-5220.202411004

Effect of SiO_2 Nanoparticles on Durability of Polyurethane-Coated Polyamide Tent Fabric

AFRIDA Noboni Rawnak[1], WANG Yiming[1], ZHOU Chuan[1], WEN Qingwen[1], LI Ni[1*], SHAO Xiaoqiang[2]
1. College of Textile Science and Engineering, Zhejiang Sci-Tech University, Hangzhou 310018, China
2. Huzhou Universal Gravity Outdoor Technology Co., Ltd., Huzhou 313099, China

Abstract: In this paper, polyamide (PA) woven fabric was used as the base fabric, and polyurethane (PU) solution containing silica nanoparticles (PU@SiO_2NPs) was used as the coating solution to prepare composite tent fabric (PA/PU@SiO_2). The morphology, structure, and durability of the tent fabric under ultraviolet (UV) radiation, water-stained, or thermal conditions were investigated. The results show that compared with PA/PU fabric without SiO_2NPs, when the mass fraction of SiO_2NPs in PU coating is 5%, the air permeability of PA/PU@SiO_2 fabric decreases from about 7.5 to 6.0 nm/s, while the reflectivity to UV-visible light is significantly improved. The surface wettability decreases, as indicated by the average water contact angle (WCA) on PA/PU@SiO_2 remaining stable at 47° after 9 min. After thermal treatment, the PA/PU@SiO_2 fabric shows superior mechanical stability. The degradation rate of the tensile strength is only 6.3%, approximately half that of the PA/PU fabric. Meanwhile, the elongation at break increases to 98.9%, compared to 61.8% for the PA/PU fabric.

Keywords: polyamide tent fabric; SiO_2 nanoparticle; polyurethane coating; durability
CLC number: TS195.2 **Document code**: A
Article ID: 1672-5220(2025)06-0620-08

Open Science Identity (OSID)

0 Introduction

With the increased life rhythm and pressure, going outside into nature becomes more and more popular for people. Thus, the demand for tourism tents increases greatly. At present, most research work for tourism tents is focused on the functional design[1]. For example, Bian et al.[2] designed a multifunctional tent, featuring a stable, convenient, energy-saving solar power source and an air purification device. Tang et al.[3] obtained a cotton tent fabric with waterproof and flame-retardant functions by optimizing the dosage of waterproofing agents and flame retardants. Zuo et al.[4] found that the aerogel in tent composite structures had an obvious thermal insulation effect, which effectively improved the internal thermal environment and weakened the phenomenon of tent "sunshine overheating" caused by sun exposure. Li et al.[5] selected the black glue fabric with UPF50+ and 210 D Oxford cloth with an ultraviolet (UV) light filtering rate of 99.8% to prepare a tent fabric with outstanding light shading.

Polyurethane (PU), as a commonly used coating material for tent fabrics, can be mixed with various resins or organic solvents. PU coatings exhibit resistance to a wide range of chemicals, including acids and industrial waste gases, owing to their customizable composition, which allows for the adjustment of material proportions to meet specific requirements. Thus, polyamide (PA) fabrics coated with PU (PA/PU) are widely used as tent fabrics because of their excellent mechanical properties, wear resistance, and waterproof performance. However, the PU coatings on PA fabrics are prone to being damaged under external forces, water, heat, UV radiation, and other factors[6-7]. Research on the durability of PA/PU tent fabric, particularly under thermal environments, remains limited[8-9].

Adding inorganic particles, such as TiO_2, SiO_2, and ZnO, is an effective way to improve polymer durability[10-11]. Among these inorganic particles, SiO_2 has high thermal stability. Composites formed by incorporating SiO_2 into polymers demonstrate excellent mechanical properties, moisture permeability, and radiative cooling performance[12-13]. In addition, SiO_2 and polymers can produce synergistic effects, endowing composite materials with new properties[14]. Zhang et al.[15] synthesized SiO_2 nanoparticles (SiO_2NPs) on the surface of aromatic PA fibers to improve the UV resistance, thermal stability, and interfacial shear strength. In our previous studies, SiO_2NPs were grafted onto PU nanofibrous membranes, which endowed the membranes with sunlight shielding performance[16-17]. The reflectivity of the PU nanofibrous membrane in the solar spectrum effectively came to 88.29%[18].

In this research, SiO_2NPs were synthesized and

Received date: 2024-11-05
* Correspondence should be addressed to LI Ni, email: lini@zstu.edu.cn
Citation: AFRIDA N R, WANG Y M, ZHOU C, et al. Effect of SiO_2 nanoparticles on durability of polyurethane-coated polyamide tent fabric [J]. *Journal of Donghua University (English Edition)*, 2025, 42(6): 620-627.

added into the PU solution to prepare a composite coating (PU@SiO_2NPs), and then the PA/PU@SiO_2 tent fabric was prepared by coating PU@SiO_2NPs on the PA fabric. The morphology, structure, and durability of the tent fabric under UV radiation, water-stained, or thermal conditions were studied, providing experimental references for the preparation and functional modification of durable tent fabrics in the future.

1 Materials and Methods

1.1 Materials

PA6 fabric (plain weave, with a yarn diameter of about 300 μm, a yarn density of 32.55 yarns/cm^2 and an area density of 60 g/m^2) was obtained from Huzhou Universal Gravity Outdoor Technology Co., Ltd., China; PU (with a commercial name of 1180A) was purchased from Shanghai Jingjian Plastic Co., Ltd., China; *N*,*N*-dimethylformamide (DMF), $NH_3 \cdot H_2O$ (with an ammonia mass fraction of 25%−28%) and anhydrous ethanol (EtOH) were purchased from Hangzhou Gaojing Fine Chemical Co., Ltd., China; tetraethyl silicate (TEOS) was purchased from Tianjin Kemi Chemical Reagent Co., Ltd., China.

1.2 Synthesis of SiO_2NPs

The stäber method was used to synthesize SiO_2NPs. Firstly, 4.40 mL TEOS was dissolved in 41.10 mL ETOH and stirred for 5 min to obtain solution A. Then, 0.95 mL $NH_3 \cdot H_2O$ was mixed with 3.55 mL deionized water and stirred for 10 min to obtain solution B. Solution A and solution B were mixed and poured into a reactor containing a polytetrafluoroethylene (PTFE) liner, and reacted at 45 ℃ for 30 min. The reaction mixture was poured into a beaker and dried in an oven (DHG-9030A, Shanghai Zhiyi Instrument Co., Ltd., China) until the solvent evaporated completely. Finally, SiO_2NPs were prepared by grinding the above reaction products in an agate mortar at a relative humidity of 65% and 25 ℃ for 10 min.

1.3 Preparation of PA/PU@SiO_2 tent fabric

Firstly, 2 g PU particles were dissolved in 8 g DMF solvent, and the PU solution was stirred for 12 h under the action of a magnetic stirrer. Then, the PU@SiO_2NP solution was prepared by dissolving SiO_2NPs in the PU solution. The effect of the SiO_2NP mass fraction w was investigated, and the mass fractions required in the coating were 1%, 3%, 5% and 7%, respectively. Finally, the PU@SiO_2NP solution was coated onto the surface of the PA fabric by using a coating machine and dried at 50 ℃ for 5 min in the oven to obtain the PA/PU@SiO_2 fabric. The thickness that the machine could coat every time was 30 μm. The coating was repeated 2−3 times until the coating was evenly distributed on the surface of the fabric. The fabric samples coated with different mass fractions of SiO_2NPs were noted as PA/PU@SiO_2-w. The preparation process of the PA/PU@SiO_2 tent fabric is shown in Fig. 1.

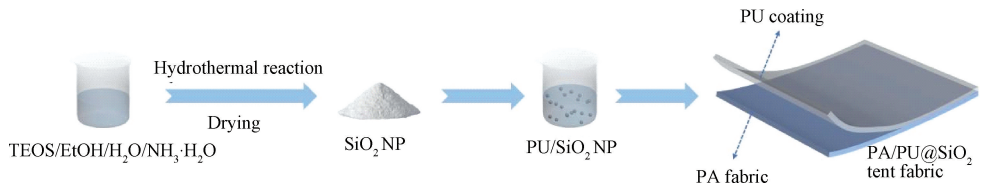

Fig. 1 Preparation process of PA/PU@SiO_2 tent fabric

1.4 Characterization

The morphology and surface elements of the samples were investigated by using a field emission scanning electron microscope (Vltra55, Carl Zeiss Company, Germany) and an energy dispersive X-ray spectroscope (A8 Advance, Brook AXS Ltd., Germany). The functional groups on macromolecular chains were analyzed by a Fourier transform infrared (FTIR) spectrometer (Nicolet 5700, Thermo Fisher Ltd., USA), with a testing wavenumber range of 4 000−500 cm^{-1}.

The air permeability of the samples was tested by using a fully automatic air permeability meter (YG461E, Wenzhou Fangyuan Instrument Co., Ltd., China), with a test pressure difference of 200 Pa and a test area of 20 cm^2. To evaluate the durability under the water-stained condition, the water contact angles (WCAs) of the samples were measured by using a contact angle measuring instrument (JCY, Shanghai Fangrui Instrument Co., Ltd., China). The volume of water droplets dropped on the surface of the sample was 3 μL. The evolution of the WCA was analyzed based on images obtained at 0, 1, 3, 7, and 9 min.

To evaluate the durability of different tent fabrics under UV radiation, the effect of UV on the PA/PU fabric and the PA/PU@SiO_2 fabric was investigated by testing their UV absorption and UV-visible (Vis) light reflection spectra with a UV-Vis near-infrared (UV-Vis-NIR) spectrophotometer (UH4150, Hitachi Ltd., Japan). To evaluate the thermal durability, the PA/PU fabric and the PA/PU@SiO_2 fabric were treated in the oven at 60 ℃ for 12 h. Then the tensile strength and the elongation at break of the samples were tested by an electronic universal testing machine (YG026D, Wenzhou Fangyuan Instrument Co., China). Samples used for tensile strength testing were rectangular with a length of 30 cm and a width of 5 cm. A constant stretching speed of 100 mm/min was applied. The averaged result of five parallel tests was recorded for each sample.

2 Results and Discussion

2.1 Morphology

Figure 2(a) shows the scanning electron microscopy (SEM) image of SiO_2NPs. It can be seen that the particles present a spherical shape with an average particle size of 100 nm. Figure 2(b) shows the SEM image of the PA fiber, revealing that the surface of the uncoated PA fiber is smooth. While for the PA/PU@SiO_2 fabric, the surface is completely covered with the coating, and the gaps between the fibers disappear. The PA fibers become indistinct, with no obvious particles observed, as shown in Fig. 2(c). The Si element mapping from the energy dispersive X-ray spectroscopy (EDS) analysis (Fig. 2(d)) shows that the Si element is evenly distributed on the fabric surface without obvious agglomeration, confirming the successful incorporation of SiO_2NPs on the fabric surface.

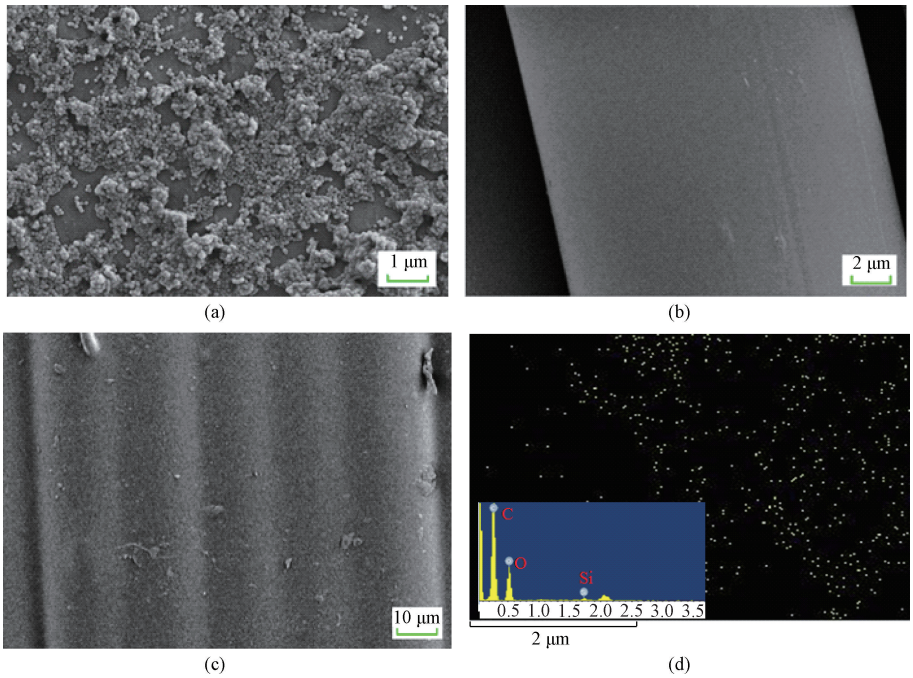

Fig. 2 SEM images and EDS spectrum: (a) SEM image of SiO_2NPs; (b) SEM image of PA fiber; (c) SEM image of PA/PU@SiO_2 fabric; (d) Si element mapping and EDS survey spectrum of PA/PU@SiO_2 fabric

2.2 Functional group

Figure 3 shows the FTIR spectra of different fabric samples. It can be seen from the FTIR spectrum of the PA fabric that characteristic peaks of PA are observed, namely the N—H stretching vibration peak at 3300 cm^{-1}, the C—H stretching vibration peak at 2 900 cm^{-1}, the amide band Ⅰ (C═O stretching vibration) at 1 640 cm^{-1} and the amide band Ⅱ (N—H bending vibration) at 1 540 and 690 cm^{-1}[18]. The FTIR spectra of PA fabrics coated with PU@SiO_2NPs show a characteristic absorption peak at 1 730 cm^{-1}. This peak is attributed to the C═O stretching vibration of the carbamate group, confirming the presence of the PU coating[19]. The FTIR spectra of the PA/PU@SiO_2 fabric samples exhibit characteristic peaks at 1 080 cm^{-1} and 800 cm^{-1}, which are assigned to the Si—O—Si symmetric stretching and bending vibration, respectively. This confirms the successful incorporation of SiO_2NPs onto the fabric surface. Meanwhile, with the increase of the mass fraction of SiO_2NPs in PU coating, the FTIR spectra show no significant change. Compared with the PA fabric, the characteristic peaks of PA in PA/PU@SiO_2 fabric spectra remain unchanged in position. Although the intensity of these peaks is not identical, the slight variation is attributed to hydrogen bonding.

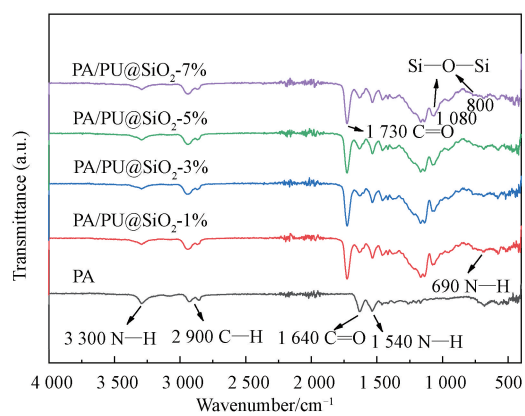

Fig. 3 FTIR spectra of PA and PA/PU@SiO_2 fabrics

2.3 Air permeability

Generally speaking, the air permeability of the fabric depends on the porosity. Although the air permeability of

the PA fiber is inferior to that of natural fibers, it is still among the better-performing synthetic fibers[20]. The air permeability of the PA fabric used in this research is approximately 450.0 nm/s. After PU coating, the air permeability of the sample significantly decreases, as shown in Fig. 4. It is probably due to the blockage of the pores between yarns and the gaps between fibers in the PA fabric (Fig. 2(c)). When the mass fraction of SiO_2NPs in PU coating is 1%, the air permeability of the PA/PU@SiO_2 fabric also decreases because of the further filling of the pores by these SiO_2NPs. It can also be found that a continuous increase in the mass fraction of SiO_2NPs does not obviously affect the air permeability of the samples.

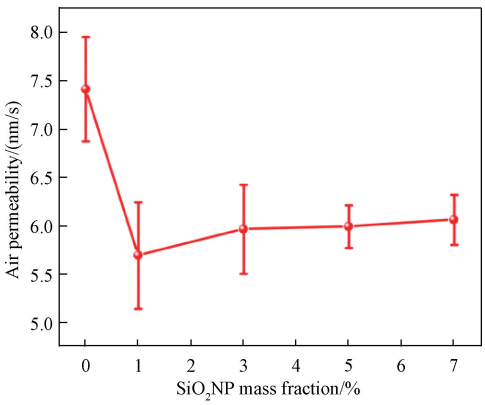

Fig. 4 Air permeability of PA/PU@SiO_2 fabrics

2.4 UV absorption and UV-Vis reflection

Figure 5 shows the UV absorption spectra and the UV-Vis reflection spectra of different samples. From Fig. 5(a), it can be seen that when the UV wavelength is shorter than 280 nm, the absorption of UV radiation by the pure PA fabric is higher than that by PA/PU or PA/PU@SiO_2 fabrics. The reason is that the functional groups on PA macromolecular chains are sensitive to UV radiation, while these groups are encapsulated by outside coating for PA/PU and PA/PU@SiO_2 fabrics[21]. In the 280–400 nm range, PA/PU and PA/PU@SiO_2 fabrics exhibit higher UV absorption than PA fabric. This is due to the sensitivity of functional groups on PU macromolecular chains to radiation within this wavelength band[22]. However, the UV absorption of PA/PU@SiO_2 fabrics shows no significant variation with changes in the mass fraction of SiO_2NPs. In summary, PU is the main contributor to UV radiation absorption across the 280–400 nm range in PA/PU@SiO_2 fabrics.

From Fig. 5(b), it can be seen that compared with the PA/PU fabric, the addition of SiO_2NPs to PU significantly improves the reflection effect of the sample in the UV-Vis range due to the amorphous micro-structure of SiO_2NPs and the presence of a high amount of silanol groups on the particle surface[23-26]. Especially, when the mass fraction of SiO_2NPs is 5%, the reflectance of UV radiation by the fabric is greatly enhanced in the UV-Vis band. Therefore, we conclude that SiO_2NPs have a minimal effect on the UV absorption of PA/PU@SiO_2 fabrics but significantly enhance the reflection of visible light. This combined effect mitigates the damage from UV-Vis radiation and thereby improves the fabrics' durability.

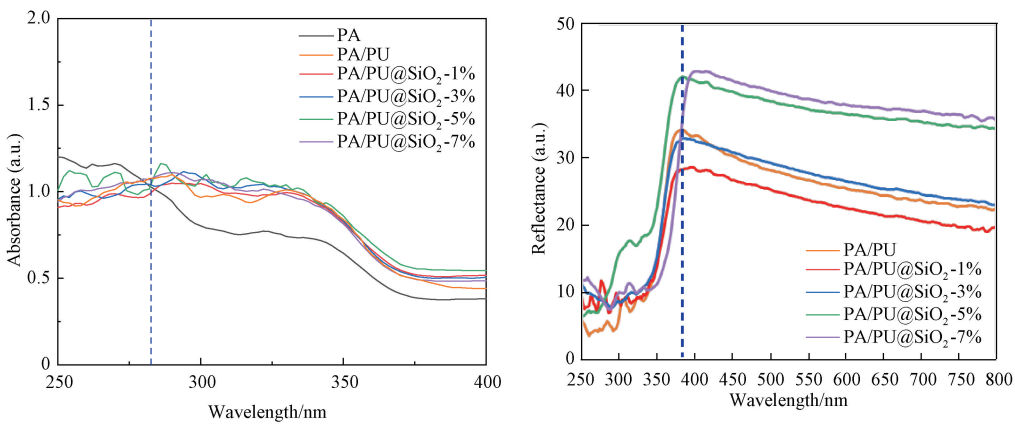

Fig. 5 UV absorption and UV-Vis reflection spectra of PA and PA/PU@SiO_2 fabrics: (a) UV absorption; (b) UV-Vis reflection

2.5 Surface wettability

Material durability under water-stained condition is mainly relative to its surface wettability. Figure 6 shows the WCA of each sample. When a water droplet is deposited on the surface of the PA fabric, the initial average WCA is 113°, indicating a hydrophobic behavior. However, unlike the other samples, the droplet rapidly wicks into the PA fabric due to its porous structure, causing a sharp decline in the WCA. After 5 min, the WCA drops to 83°. After 9 min, the water fully penetrates the PA fabric, at which point the WCA reaches 0°.

When PU is coated on the surface of the PA fabric, the hydrophobicity of the sample surface is weakened due to the presence of hydrophilic groups on the PU polymer chains. When a water droplet is deposited on the surface of the PA/PU fabric, the initial average WCA is 104°,

which is smaller than that of the PA fabric. However, the decrease of the WCA with the time on the PA/PU fabric is slower because the pores on the PA fabric surface are filled by PU coating (Fig. 2(c)). After 5 min, the WCA is almost the same as that of the PA fabric. After 9 min, the WCA remains at 62°, indicating weakened surface wettability.

Due to the lack of hydrophobic treatment to the added SiO_2NPs, there are a large number of —OH functional groups on the surface of SiO_2NPs. Therefore, when SiO_2NPs are added to the PU coating, compared with the PA/PU fabric, the WCAs of the PA/PU@SiO_2 fabrics decrease further. However, PA/PU@SiO_2 fabrics present a similar wettability persistence with the PA/PU fabric. After 9 min, the WCAs of PA/PU@SiO_2 fabrics with SiO_2NP mass fractions of 5% and 7% are 47°. In our future work, SiO_2NPs would be chemically modified to enhance the hydrophobicity and to reduce the surface wettability of PA/PU@SiO_2 fabrics, thus improving fabric durability under moisture or water-stained conditions.

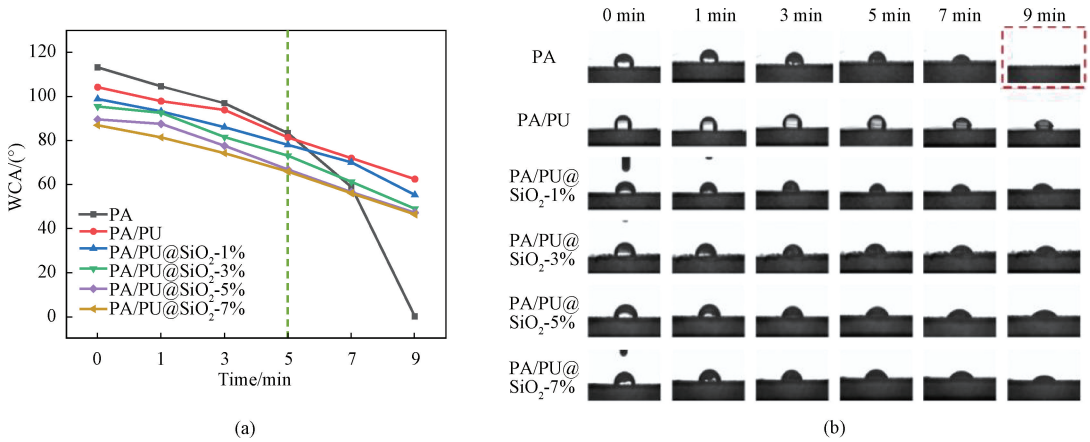

(a) (b)

Fig. 6 WCAs of PA, PA/PU and PA/PU@SiO_2 fabrics: (a) WACs; (b) images of WCAs

2.6 Mechanical property

The mechanical properties of various samples before and after thermal treatment are shown in Fig. 7.

Figure 7(a) shows that with the increasing SiO_2NP mass fraction, both the tensile strength and elongation at break of the samples peak at a SiO_2NP mass fraction of 5%. When SiO_2NPs are added to the PU coating, these nanoparticles can also endure an external force partly. The mechanical properties are improved by the addition of SiO_2NPs. The observed phenomenon can be attributed to three factors: hydrogen bonding between Si—OH groups, the low free energy of the long-chain organic silane on the SiO_2NP surface, and interactions between the PU and PA macromolecular chains. However, at higher mass fractions, the SiO_2NPs tend to aggregate. When the mass fraction reaches 7%, this aggregation becomes significant enough to cause stress concentration in the PU coating, ultimately resulting in the observed decrease in both tensile strength and elongation at break.

Figure 7(b) shows the changes of the mechanical properties of the samples after thermal treatment at 60 ℃ for 12 h. Due to the stress relaxation and the shrinkage of the PU and PA macro-molecular chains under the action of heat, the tensile strength of each sample decreases slightly, and the elongation at break increases slightly compared to that of the samples before thermal treatment. For the PA/PU fabric, the tensile strength before thermal treatment is 624 N, and the elongation at break is 37.3% (Fig. 7(a)). After thermal treatment, the strength decreases to 538 N, and the elongation increases to 52.7%. When the mass fraction of SiO_2NPs is 5%, the tensile strength of the sample before thermal treatment is 714 N, and the elongation at break is 61.8%. After thermal treatment, the strength decreases to 669 N, and the elongation at break increases to 98.9%. The difference of tensile strength of all samples before and after thermal treatment is shown in Fig. 7(c) with blue bars (note that the bars represent the absolute value of the change, corresponding to a net reduction in tensile strength). The difference decreases with the increase of the mass fraction of SiO_2NPs, and when the mass fraction comes to 5%, the tensile strength attenuation is the smallest. At this time, the difference of the elongation at break with the red bars is conversely the largest. This is because SiO_2NPs possess high thermal stability and excellent thermal conductivity[27]. As shown in Fig. 7(d), this facilitates rapid heat dissipation, which prevents heat accumulation in the PU coating on the PA fabric. Consequently, the thermal degradation rate of both the PU coating and the overall PA/PU fabric is reduced.

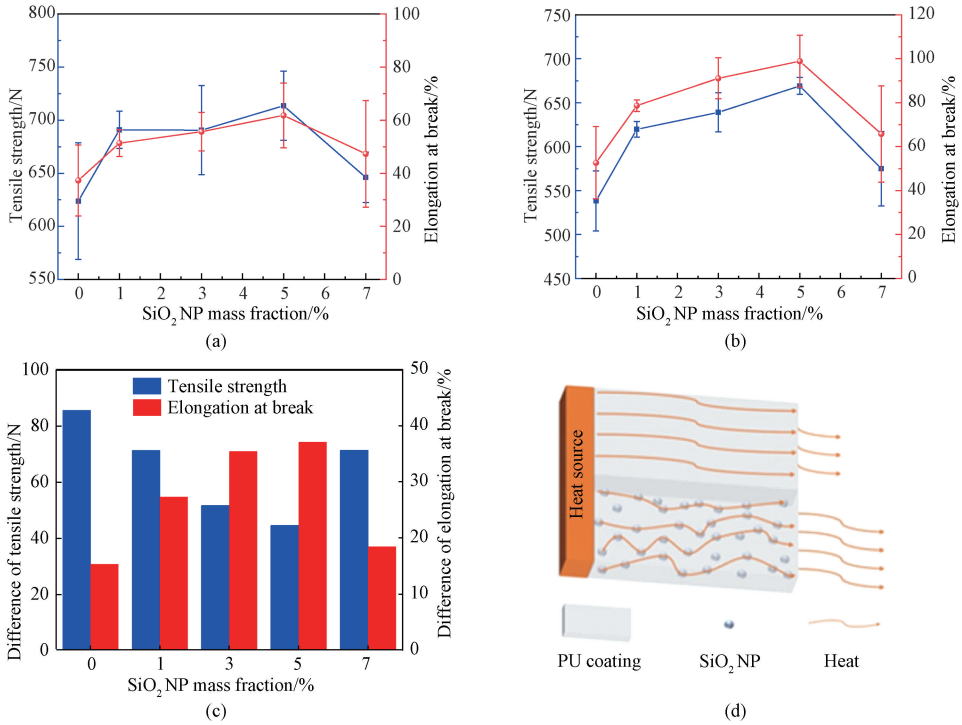

Fig. 7 Mechanical properties of PA/PU@SiO_2 fabrics: (a) before thermal treatment; (b) after thermal treatment; (c) difference of tensile strength and elongation at break before and after thermal treatment; (d) illustration of heat dissipation in PU coating

3 Conclusions

This study fabricated PA/PU@SiO_2 fabrics by coating the PA base fabric with PU solutions containing SiO_2NPs. We investigated the influence of the mass fraction of SiO_2NPs on key properties of the fabrics, including air permeability, UV absorption, UV-Vis reflection, surface wettability, and mechanical performance. The results demonstrate that the fabric containing a mass fraction of 5% SiO_2NPs exhibit the optimal combination of UV absorption and UV-Vis light reflection. Furthermore, this fabric retains a WCA of 47° even after 9 min. After thermal treatment at 60 ℃ for 12 h, its tensile strength decreases by only 6.3% (from 714 to 669 N), while the elongation at break increases from 61.8% to 98.9%. In conclusion, PA/PU@SiO_2 fabrics exhibit comprehensively improved durability, showing great promise for application as high-performance tent fabrics.

References

[1] WANG Y P. Functionality and detection analysis of coated fabrics for tents [J]. *Heilongjiang Science and Technology Information*, 2017, 15: 23. (in Chinese)

[2] BIAN Z, ZHANG Y L, ZHU X D, et al. Design of multi-functional relief tents [J]. *Journal of Jiamusi University (Natural Science Edition)*, 2017, 35(4): 590-592. (in Chinese)

[3] TANG L, LI M, LIU J W, et al. Preparation and performance of flame retardant and waterproof cotton tent fabric[J]. *China Dyeing & Finishing*, 2023, 49(11): 53-56. (in Chinese)

[4] ZUO X B, SONG Y, FAN K X, et al. Comparative of thermal insulation materials in tent[J]. *Building Energy & Environment*, 2022, 41(9): 56-59. (in Chinese)

[5] LI H J, GU H Y. Sunshade-equipped tent: CN215889552U[P]. 2022-02-22. (in Chinese)

[6] YANG Y M, CAO H, LIU R L, et al. Fabrication of ultraviolet resistant and anti-bacterial non-isocyanate polyurethanes using the oligomers from the reductive catalytic fractionated lignin oil [J]. *Industrial Crops and Products*, 2023, 193: 116213.

[7] SHEN Y, LIU J, LI Z, et al. UV-curable organic silicone grafting modified waterborne polyurethane acrylate: preparation and properties [J]. *International Journal of Adhesion and Adhesives*, 2024, 129: 103583.

[8] WEN Y, LUO Q, CHEN J, et al. Aging mechanism and property of PU contained polybutadiene and its hydrogenated soft segment [J]. *New Chemical Materials*, 2020, 48(6): 203-207. (in Chinese)

[9] CUI X L, DONG Q X, QIU P, et al. Research

progress on aging mechanism and life prediction of polyurethane[J]. *Railway Engineering*, 2023, 63(8): 141-144. (in Chinese)

[10] HUANG J, ZHANG F Y, WANG X, et al. Preparation of heat insulation light coating tent cloth[J]. *Tianjin Textile Science & Technology*, 2021(4): 55-59. (in Chinese)

[11] PAN Y Q, LIU J Z, GONG L, et al. Reducing light scattering of single-layer TiO_2 and single-layer SiO_2 optical thin films[J]. *Optik*, 2021, 231: 166380.

[12] PAN X X, ZHU Y W, LIU L D, et al. Multifunctional polyacrylonitrile-SiO_2/TiO_2 hollow particle nanofibrous membranes with robust ultraviolet resistance and antibacterial effect[J]. *Chemical Communications*, 2024, 60(82): 11758-11761.

[13] GU H H, LI G Q, LI P P, et al. Superhydrophobic and breathable SiO_2/polyurethane porous membrane for durable water repellent application and oil-water separation[J]. *Applied Surface Science*, 2020, 512: 144837.

[14] ZHENG J C, LIU J D, MENG Z, et al. Surface treatment of silica and its application in polyamide 6 [J]. *Engineering Plastics Application*, 2023, 51(1): 115-122. (in Chinese)

[15] ZHANG L W, KONG H J, QIAO M M, et al. Growing nano-SiO_2 on the surface of aramid fibers assisted by supercritical CO_2 to enhance the thermal stability, interfacial shear strength, and UV resistance [J]. *Polymers*, 2019, 11(9): 1397.

[16] LIU R, ZHOU C, WANG Y M, et al. In-situ grown SiO_2 on amino-silane modified polyacrylonitrile nanofibrous membranes and its waterproof-breathable and light-shielding properties[J]. *Applied Surface Science*, 2024, 642: 158536.

[17] WANG H J, CHEN L, YI Y Q, et al. Durable polyurethane/SiO_2 nanofibrous membranes by electrospinning for waterproof and breathable textiles[J]. *ACS Applied Nano Materials*, 2022, 5(8): 10686-10695.

[18] WANG H J, ZHOU C, WANG Y M, et al. Polyurethane-SiO_2 tandem composite fibrous membrane for passive daytime radiative cooling [J]. *Solar Energy Materials and Solar Cells*, 2025, 279: 113244.

[19] WANG H J. Preparation of silica modified polyurethane nanofiber membrane and study on the waterproof and breathable properties [D]. Hangzhou: Zhejiang Sci-Tech University, 2023. (in Chinese)

[20] GO C W, YANG J H, KWAK D S, et al. Waterborne polyurethane modified with silicone macromer and the nylon airbag coated with it [J]. *Textile Research Journal*, 2016, 86(19): 2015-2021.

[21] DU S, WEI Y H, AHMED S, et al. Enhanced thermal stability and UV resistance of polyamide 6 filament fabric via in situ grafting with methyl methacrylate [J]. *Colloids and Surfaces A: Physicochemical and Engineering Aspects*, 2022, 651: 129371.

[22] JIN W J, HE W L, CHENG S S, et al. Highly sticky caramel modified coating for multifunctional polyamide 6 fabric: UV blocking, anti-bacterial and flame retardancy[J]. *Progress in Organic Coatings*, 2024, 194: 108563.

[23] KATANGUR P, PATRA P K, WARNER S B. Nanostructured ultraviolet resistant polymer coatings[J]. *Polymer Degradation and Stability*, 2006, 91(10): 2437-2442.

[24] ESLAMI R, BAGHERI R, HASHEMZADEH Y, et al. Optical and mechanical properties of transparent acrylic based polyurethane nano silica composite coatings [J]. *Progress in Organic Coatings*, 2014, 77(7): 1184-1190.

[25] ZEMLYANSKII V S, STEPANCHUK A A, SYCHEV M M, et al. Influence of the structure of the surface layer of silica glass on the radiation losses in the UV spectral range[J]. *Glass Physics and Chemistry*, 2008, 34(3): 248-254.

[26] SARAVANAN S, DUBEY R S. Fabrication and characterization of TiO_2/SiO_2 multilayers using sol-gel spin coating method [J]. *Nanosystems: Physics, Chemistry, Mathematics*, 2019, 10(1): 63-69.

[27] JIA Y, MAO Z P, HUANG W X, et al. Effect of temperature and crystallinity on the thermal conductivity of semi-crystalline polymers: a case study of polyethylene [J]. *Materials Chemistry and Physics*, 2022, 287: 126325.

SiO_2纳米颗粒对聚氨酯涂层聚酰胺帐篷织物耐用性能的影响

AFRIDA Noboni Rawnak[1]，王祎铭[1]，周　川[1]，温晴雯[1]，李　妮[1*]，邵晓强[2]

1. 浙江理工大学纺织科学与工程学院，浙江 杭州 310018

2. 湖州万有引力户外科技有限公司，浙江 湖州 313099

摘　要：以聚酰胺（polyamide，PA）机织物为基布，以含有 SiO_2 纳米颗粒（SiO_2NPs）的聚氨酯溶液为涂层溶液（PU@SiO_2NPs），制备了复合帐篷织物（PA/PU@SiO_2）。研究了该帐篷织物的形态结构，以及在紫外线照射、沾水和热环境中的耐用性能。结果表明，与不含 SiO_2NPs 的织物相比，当聚氨酯涂层中 SiO_2NPs 的质量分数为 5%时，虽然 PA/PU@SiO_2 织物的透气率从约 7.5 nm/s 降低到 6.0 nm/s，但对紫外可见光的反射率显著提高，且织物表面润湿性减弱，9 min 后 PA/PU@SiO_2 织物上的平均水接触角仍保持在 47°。热老化处理后，PA/PU@SiO_2 织物的拉伸强力损失率为 6.3%，约为 PA/PU 织物热老化处理后拉伸强力损失率的一半，PA/PU@SiO_2 织物断裂伸长率从 PA/PU 织物的 61.8%增加到 98.9%。

关键词：聚酰胺帐篷织物；SiO_2 纳米颗粒；聚氨酯涂层；耐用性能